Journal of Biomedical Optics 7(3), 435–441 (July 2002)

Raman scattering anisotropy of biological systems

Masamichi Tsuboi
Iwaki-Meisei University
College of Science and Engineering
Iwaki, Fukushima 970-8551, Japan

Abstract. Raman scattering from membranes, cells, and tissues must all be anisotropic, because the molecular orientations in these biological systems are anisotropic. How can such observed Raman scattering anisotropy be related with a biologically relevant molecular arrangement? This question is the subject of this paper. A general method of addressing this question will be given, with three examples illustrating the use of the method: (1) carotenoid arrangement in the eyespot of *Chlamydomonas*, (2) orientation of the tryptophan side chain in the coat subunit of a filamentous virus, and (3) polypeptide orientation in fowl feather barb. [DOI: 10.1117/1.1482720]

Keywords: Raman scattering anisotropy; eyespot of *Chlamydomonas*; tryptophan side chain; filamentous virus; fowl feather barb.

Paper JBO 01008 received Jan. 25, 2001; revised manuscript received Jan. 4, 2002; accepted for publication Feb. 7, 2002.

Introduction

Many of the molecules involved in a living cell or a tissue have some regular, fixed arrangements that are relevant to their biological functions. By use of a Raman microscope, we can now obtain Raman scattering from an area of the subject's system as small as 1 μm^2. By use of a polarizer, in addition, we can observe anisotropy of such Raman scattering, and this must be related to the regular orientation of a certain molecule in that small area. Such a relation is well known in principle. In bringing the principle into practice dealing with a biological sample, however, we encounter a number of problems to be solved. In this paper, a general method will be given stepwise as to how to relate observed Raman scattering anisotropy to the orientation of a molecule in a given biological system. For each step some examples will be shown. In conclusion, it will be shown that the examination of Raman scattering anisotropy can lead to unique and significant information on the local structure of a biological system.

General Method

A series of procedures for determining the orientation of a molecule in a biological system is described below step by step.

Step 1. Assign a proper rectangular coordinate axis system (*abc*) to the biological system in question. For the *Chlamydomonas* cell, for example, the axes are defined as shown in Figure 1. The shape of this cell is a slightly prolate ellipsoid of about 10 μm in diameter. The *c* axis, or the cell axis, is defined as the bisector of the two flagella that project outward from the cell surface. This happens to coincide with the long axis of the ellipsoid (Figure 1). The eyespot of *Chlamydomonas* is known to be located near the surface on the ''equator,'' i.e., at the farthest point from the meridian or the cell axis (*c* axis).[1] The *b* axis is defined as perpendicular to the *c* axis and to involve this eyespot (Figure 1), and the *a* axis is perpendicular to the *bc* plane.

Address all correspondence to Masamichi Tsuboi. Tel: +81-246-29-5111 ext. 653; Fax: +81-246-29-0577; E-mail: tsuboima@iwakimu.ac.jp

Step 2. Choose a Raman band assignable to a known vibration of the molecule. Establish the Raman scattering tensor of the Raman band for the given excitation wavelength.[2] The tensor should have a set of principal axes (*xyz*) and three nonzero components, α_{xx}, α_{yy}, and α_{zz}. It is not usually easy to establish the absolute values of these three tensor components. It is sufficient, however, to fix their relative magnitudes: $r_1 = \alpha_{xx}/\alpha_{zz}$ and $r_2 = \alpha_{yy}/\alpha_{zz}$.

Step 3. By use of a Raman microscope, in combination with a Raman mapping system, the distribution of the Raman intensity should be determined within an appropriate range of the (*abc*) coordinates. For the *Chlamydomonas* cell, for example, the 1530 cm^{-1} band of the carotenoid pigment (excited at 488.0 nm) was found to be very intense in a small elongated volume of $1\times1\times2$ μm^2, which coincided with the location of the eyespot (Figure 2).

Step 4. Our current goal is to determine the orientation of the (*xyz*) cordinate system (Raman tensor) with respect to the (*abc*) coordinate system (cell or tissue) at a particular spot in the (*abc*) coordinate system. For this, the Raman scattering intensities, *Iaa*, *Ibb*, *Icc*, *Iab*, *Ibc*, and *Iac* are measured for the Raman band in question at the particular spot. Here, *Iab* means, for example, that the electric vector of the exciting beam is placed along the *a* axis, and the electric vector of the scattering beam is placed along the *b* axis.

Step 5. In this step, a formulation is established to relate observed *Iaa*, *Ibb*, *Icc*, *Iab*, *Ibc*, and *Iac* with tensor components α_{xx}, α_{yy}, and α_{zz}. Eulerian angles, θ, ϕ, and χ, that describe the orientation of the (*xyz*) axes in the (*abc*) coordinate system are chosen (shown in Figure 3). Here, θ and ϕ are the ordinary polar coordinates of the *z* axis in the (*abc*) system and χ is an angle in the *xy* plane that measures the rotation about the *z* axis.[3] Direction cosines of the *x*, *y*, and *z* axes in the (*abc*) axis system are given as functions of Eulerian angles:

$$l_x = \cos\theta\cos\phi\cos\chi - \sin\phi\sin\chi, \qquad (1a)$$

1083-3668/2002/$15.00 © 2002 SPIE

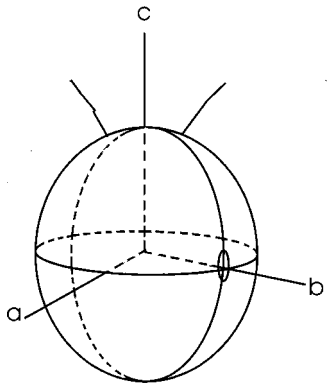

Fig. 1 Definitions of the *a*, *b*, and *c* axes for the *Chlamydomonas* cell. The small ellipse, along the *b* axis, indicates the location of the eyespot.

$$m_x = \cos\theta \sin\phi \cos\chi + \cos\phi \sin\chi, \tag{1b}$$

$$n_x = -\sin\theta \cos\chi, \tag{1c}$$

$$l_y = -\cos\theta \cos\phi \sin\chi - \sin\phi \cos\chi, \tag{1d}$$

$$m_y = -\cos\theta \sin\phi \sin\chi + \cos\theta \cos\chi, \tag{1e}$$

$$n_y = \sin\theta \sin\chi, \tag{1f}$$

$$l_z = \sin\theta \cos\phi, \tag{1g}$$

$$m_z = \sin\theta \sin\phi, \tag{1h}$$

$$n_z = \cos\theta. \tag{1i}$$

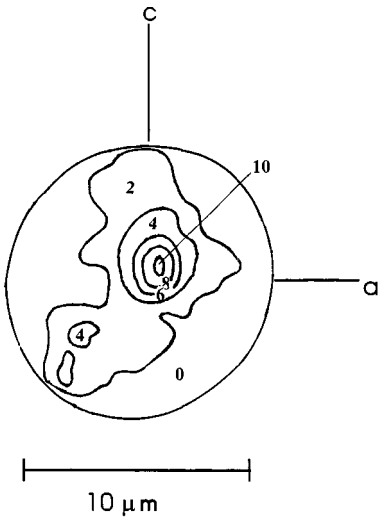

Fig. 2 Distribution of the peak intensity of the 1530 cm^{-1} Raman band in the *Chlamydomonas* cell (Ref. 4). The number in each area indicates the relative peak intensity observed in that area. This was drawn on the basis of computer output shown in Fig. 6(c) in Ref. 4.

The observed Raman scattering intensities *Iaa*, *Ibb*,…,*Iac* are the squares of the following Raman scattering tensor components.

$$\alpha_{aa} = l_x^2\alpha_{xx} + l_y^2\alpha_{yy} + l_z^2\alpha_{zz}, \tag{2a}$$

$$\alpha_{bb} = m_x^2\alpha_{xx} + m_y^2\alpha_{yy} + m_z^2\alpha_{zz}, \tag{2b}$$

$$\alpha_{cc} = n_x^2\alpha_{xx} + n_y^2\alpha_{yy} + n_z^2\alpha_{zz}, \tag{2c}$$

$$\alpha_{ab} = l_x m_x \alpha_{xx} + 1_y m_y \alpha_{yy} + l_z m_z \alpha_{zz}, \tag{2d}$$

$$\alpha_{bc} = m_x n_x \alpha_{xx} + m_y n_y \alpha_{yy} + m_z n_z \alpha'_{zz}, \tag{2e}$$

$$\alpha_{ac} = l_x n_x \alpha_{xx} + l_y n_y \alpha_{yy} + l_z n_z \alpha_{zz}. \tag{2f}$$

As noted above, only the relative magnitudes of the tensor components ($r_1 = \alpha_{xx}/\alpha_{zz}$ and $r_2 = \alpha_{yy}/\alpha_{zz}$) are usually investigated, and only the Raman intensity ratios, rather than the absolute intensities, are measured. Therefore, Eqs. (2a)–(2f) are in practice replaced by relationships of the form,

$$Iaa/Ibb = (\alpha_{aa}/\alpha_{bb})^2 = (l_x^2 r_1 + l_y^2 r_2 + l_z^2)^2/(m_x^2 r_1 + m_y^2 r_2 + m_z^2)^2. \tag{3}$$

Similar equations hold for other polarized Raman intensity ratios, *Ibb*/*Icc*, *Ibc*/*Icc*, *Iac*/*Icc*, and *Iab*/*Iaa*, *mutatis mutandis*.

Step 6. In the final step, the determination of the orientation angles (θ,ϕ,χ) is accomplished. This is done essentially through a trial-and-error procedure. If an arbitrary set of (θ,ϕ,χ) is assumed, direction cosines l_x, m_x, n_x, l_y, m_y, n_y, l_z, m_z, and n_z can be calculated by Eqs. (1a)–(1i), and then *Iaa*/*Ibb*, *Ibb*/*Icc*, *Ibc*/*Icc*, *Iac*/*Icc*, and *Iab*/*Iaa* can be calculated through Eq. (3) and similar equations for the polarized Raman intensity ratios. The calculated *Iaa*/*Ibb* can be compared with the observed *Iaa*/*Ibb*, and the calculated *Ibb*/*Icc* can be compared with the observed *Ibb*/*Icc*, if it is experimentally available. By a proper computer program, a number of test sets of (θ,ϕ,χ) can be examined in a systematic manner, until a satisfactory agreement is reached between the calculated set of Raman intensity ratios, *Iaa*/*Ibb*, *Ibb*/*Icc*, *Ibc*/*Icc*, *Iac*/*Icc*, and *Iab*/*Iaa* and the corresponding set of observed intensity ratios.

Special Case

Quite often, the molecular arrangement in a biological system has axial symmetry. This is the case, for example, for some filamentous bacteriophages and for fowl feather barb. In such a case, the *a* axis and *b* axis are equivalent (step 1), and only *Ibb*, *Icc*, *Ibc*, and *Iab* form an independent set of information (step 4). Step 5 is simplified as follows: The orientation of the (*xyz*) axis system in the biological system (*abc*) is given by two angles, θ and χ. *Icc*/*Ibb* is now directly expressed by θ and χ as

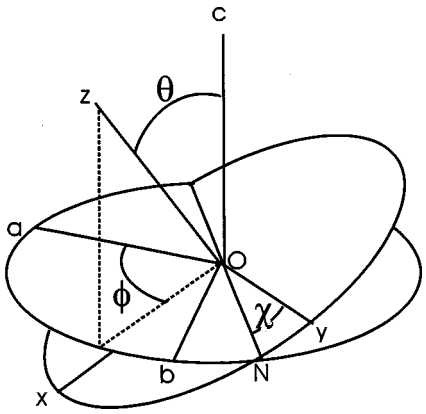

Fig. 3 Definition of Eulerian angles, θ, ϕ, and χ, which relate the coordinates (*xyz*) with (*abc*).

$$Icc/Ibb = 4[\sin^2\theta(r_1\cos^2\chi + r_2\sin^2\chi) + \cos^2\theta]^2/[\cos^2\theta(r_1\cos^2\chi + r_2\sin^2\chi) + (r_1\sin^2\chi + r_2\cos^2\chi) + \sin^2\theta]^2. \quad (4)$$

Step 6 is also simplified. By Eq. (4), Icc/Ibb is calculated for various θ and χ values, and the results are mapped in (θ, χ) space. Here, some contour lines for given Icc/Ibb values can be created by relatively simple computer programming. By examining a point of intersection of these contour lines, a common set of (θ, χ) values is found that reproduces all the observed polarized Raman intensity ratios.

Example I. Orientation of Carotenoid Molecules in the Eyespot of *Chlamydomonas*

(Step 1). The (*abc*) axes have already been defined above (Figure 1). (Step 2). Raman spectra of a single cell of *Chlamydomonas* have been examined with 488.0 nm excitation at various points within the cell. At every point, two strong bands, which are assigned to carotenoid, were observed at 1530 and 1159 cm^{-1}. (Step 3). By the use of a Raman mapping system, the intensity distribution of the 1530 cm^{-1} band was examined.[4] When the *ac* plane was placed parallel to the microscope sample stage, a map, shown in Figure 3, was obtained. On the basis of the known structure of this cell,[1,5] an elongated peak observed at its surface is considered to be the eyespot. (Step 4). At this spot, polarized Raman spectra were observed. The results are shown in Figure 4, which indicates that the polarizability oscillation caused by the 1530 cm^{-1} vibration takes place mostly along the *c* axis or mostly along the direction of elongation. For the 488.0 nm excitation, the carotenoid 1530 cm^{-1} band must be in resonance with its first electronic absorption band, whose transition moment is along the conjugated double-bond chain (*z* axis). Therefore, the Raman tensor in question is considered to have only one nonzero component, α_{zz}. Thus, it is concluded that the carotenoid molecules in the eyespot are arranged with their *z* axes (conjugated double-bond chain axes) parallel to the cell axis.

The intensity of the light, which causes a chemical reaction at the eyespot of *Chlamydomonas*, must be greatly dependent upon the orientation of this analyzer, which is directly determined by the orientation of the cell itself, with respect to the light beam as well as its polarization direction. One may speculate that the cell is detecting, through the eyespot, not only the direction of the light, but also the location of the surface of the water medium in which the cell is swimming (Figure 5).

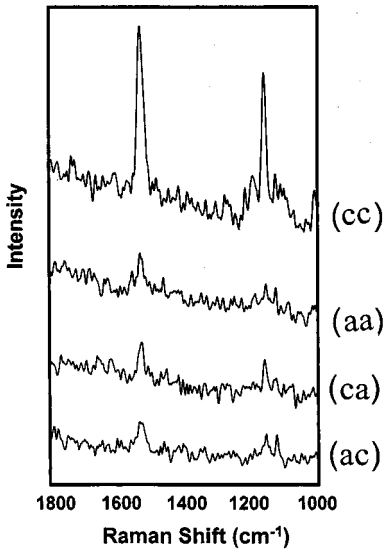

Fig. 4 Polarized Raman spectra (*cc*), (*aa*), (*ca*), and (*ac*) of the same cell as that shown in Fig. 3 at the spot with Raman intensity 10 (Ref. 4). Here (*ca*) means, for example, that the electric vector of the exciting beam is placed along the *c* axis, and that the electric vector of the scattering beam is placed along the *a* axis. This is essentially a reproduction of Fig. 7 in Ref. 4.

Example II. Orientation of the Tryptophan Residue in a Filamentous Bacteriophage

(Step 1). *fd* is a bacteriophage with the shape of a long (about 880 nm) thin (about 6 nm) cylinder. In this cylinder, a single stranded DNA loop of 6410 nucleotides is packaged within a sheath comprising about 2700 copies of a 50-residue α-helical subunit (pVIII). The cylinder has axial symmetry; its axis is chosen as the *c* axis, and the *a* and *b* axes are perpendicular to it. (Step 2). The subunit (pVIII) has one tryptophan residue (W26). In view of the importance of the tryptophan Raman bands as sources of specific information on the environment and interaction of tryptophan residues in proteins, Tsuboi

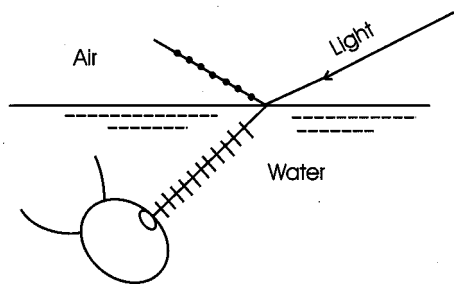

Fig. 5 *Chlamydomonas* eyespot maybe detecting the direction of polarization of the incident light beam.

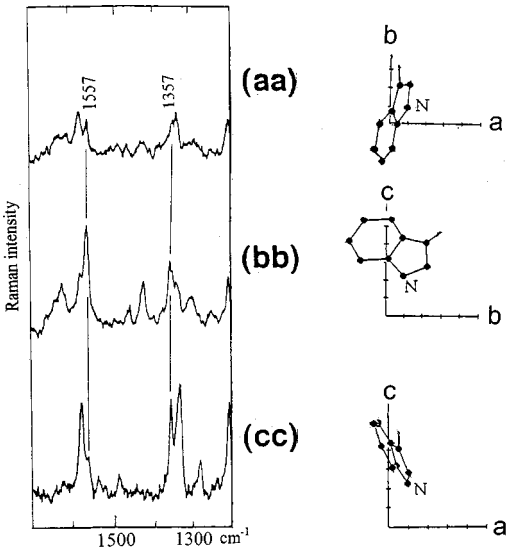

Fig. 6 Indole ring orientation (Ref. 7) and polarized Raman spectra (488.0 nm excitation) (Ref. 6) of an orthorhombic *N*-acetyl-*L*-tryptophan crystal. In each orientation the incident and scattered electric vectors are parallel to one of the crystallographic axes. On the left-hand side is a partial reproduction of Fig. 2 in Ref. 6, and on the right-hand side is a partial reproduction of Fig. 1 in Ref. 6.

et al.[6] investigated their intrinsic Raman tensors. As a model for the tryptophan residue in proteins, they employed *N*-acetyl-*L*-tryptophan, for which an x-ray crystal structure is available.[7] Polarized Raman spectra were obtained from an oriented single crystal of *N*-acetyl-*L*-tryptophan by use of a Raman microscope and 488.0 nm excitation. The crystal, of orthorhombic space group $P2_12_12_1$, provides the relative Raman intensities *Iaa*, *Ibb*, and *Icc* that correspond to *aa*, *bb*, and *cc* components of the crystal Raman tensor[6] (Figure 6). The Raman tensors derived from these intensity data are shown in Figure 7. Step 3. The virus solution (about 50 mg/mL) was drawn into an oriented fiber of about 0.5 mm thickness by slowly drawing a spherical drop between the glass rods of a fiber-pulling device which was maintained in a hygrostatic environment (92% relative humidity). Every virion particle is considered to be arranged with its *c* axis along the fiber axis.[8] Step 4. Raman scattering intensities *Icc* and *Ibb* were examined, and the results are shown in Figure 8(a). Thus

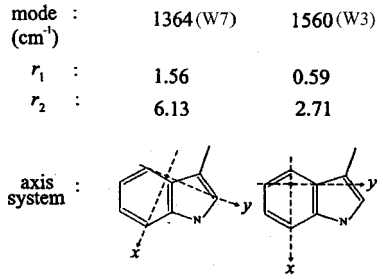

Fig. 7 Principal axes (*x*, *y*, and *z*) and Raman tensor values (r_1 and r_2) for the normal modes W7 (1357 cm^{-1}) and W3 (1557 cm^{-1}) of the indole ring of a *N*-acetyl-*L*-tryptophan single crystal (Ref. 6). This is a partial reproduction of Fig. 4 in Ref. 9.

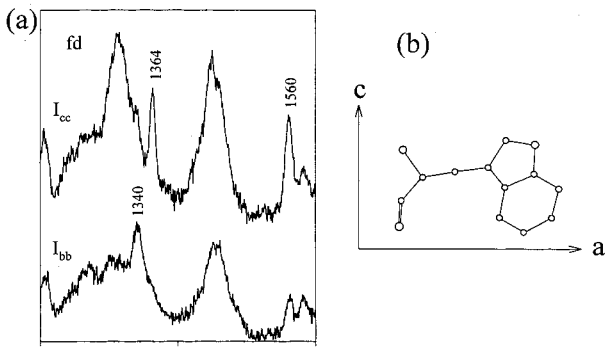

Fig. 8 (a) Polarized Raman spectra of *fd* in the 1200–1600 cm^{-1} region (Ref. 9). This is a partial reproduction of Fig. 4 in Ref. 9. (b) Illustration of the indole ring orientation of tryptophan-26 in the *fd* subunit (Ref. 9).

Icc/*Ibb* for the 1560 cm^{-1} (W3) band was found to be 2.8 $\pm$0.5 and *Icc*/*Ibb* for the 1364 cm^{-1} (W7) to be 20$\pm$5. Step 5. By the use of Eq. (4), with the r_1 and r_2 values determined in step 2, contour lines for various *Icc*/*Ibb* values were drawn in θ and χ space (Figure 9). Step 6. By projecting the observed values of *Icc*/*Ibb* onto this contour map, with their experimental errors taken into account, a probable set of values of θ and χ was estimated. The first reasonable estimate with the uncertainty in the (θ, χ) pair was (90$\pm$10°,54 $\pm$3°).[9] By taking other factors [(i)–(iv) given below] into account, however, Tsuboi et al.[9] made a slight change in the pair of (θ, χ) values. Thus, (i) the dihedral angle $\chi^{2,1}$(Cα-Cβ-C3-C2) must be around $\pm$120°, because the W3 frequency=1560 cm^{-1}. [10] (ii) The pseudo twofold axis

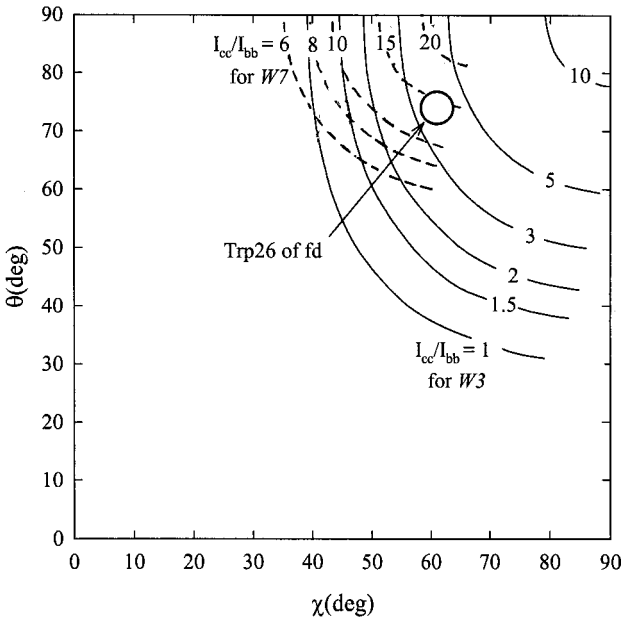

Fig. 9 Contour map of *Icc*/*Ibb* in (θ, χ) space for the tryptophan Raman bands at 1560 cm^{-1} (W3, solid lines) and at 1364 cm^{-1} (W7, broken lines) (Ref. 9). This is essentially a partial reproduction of Fig. 5(A) in Ref. 9. Details of how to construct these contour lines are given in Ref. 9.

Table 1 Revised atomic coordinates of the indole ring moiety of W26 in *fd*.[a]

Atom (*N*)	*x*	*y*	*z*
C (186)	6.555	–20.427	33.860
Cd1 (187)	7.279	–20.351	35.085
Cd2 (188)	7.240	–19.602	32.968
Ne1 (189)	8.483	–19.581	34.890
Ce2 (190)	8.436	–19.111	33.577
Ce3 (191)	7.017	–19.310	31.602
Cz2 (192)	9.467	–18.421	32.905
Cz3 (193)	8.006	–18.561	30.935
Ch2 (194)	9.166	–18.102	31.586

[a]Obtained from the atomic coordinates of atoms 186–194 of entry 1IFJ of the Protein Data Bank by rotating 15° about the Cα–Cβ bond at 179° about the Cβ–Cγ bond.

of the indole ring must be at an angle (ψ) of $38° \pm 6°$ from the virion axis on the basis of a difference in Raman linear intensity of flow-oriented *fd*.[11] (iii) The set of dihedral angles χ^1(N-Cα-Cβ-C3) and $\chi^{2,1}$(Cα-Cβ-C3-C2) must be consistent with the tryptophan side-chain rotamer library of Ponder and Richards.[12] (iv) The final model must be plausible on the basis of an energy-minimized calculation. As detailed in a previous paper,[9] the final set of orientation angles of tryptophan-26 reached is $\theta = 74°$ and $\chi = 61°$, which gives $\chi^1 = -100°$, $\chi^{2,1} = 111°$, and $\psi = 32°$, which is still in agreement with the observed Icc/Ibb values, 2.8 ± 0.5 for the 1560 cm^{-1} band and 20 ± 5 for the 1364 cm^{-1} band, within experimental error. The subunit structure of *fd* and subunit arrangement in *fd* have been investigated by Marvin and co-workers[13,14] by the x-ray fiber diffraction method, and the results are given in the Protein Data Bank (identification No. 1IFJ). From the Raman anisotropy study, the atomic coordinates of the indole ring of tryptophan-26 were proposed to have changed as shown in Table 1.

A similar study was made on another filamentous bacteriophage *Pf*3.[15] It consisted of a covalently closed single-stranded DNA genome of about 6300 nucleotides encased in a sheath comprising about 2630 copies of a 44-residue α-helical subunit. This subunit has one tryptophan (W38) in its C-terminal region. On the basis of the observed scattering anisotropy of the 1369 and 1548 cm^{-1} bands, the orientation of the indole ring of W38 with respect to the virion axis (*c* axis) was determined. The Eulerian angles were found to be $(\theta, \chi) = (73 \pm 4°, 44 \pm 3°)$. This orientation was found to be different from what was given in the model by Welsh et al.[16] (Protein Data Bank ID No. 1IFP), but it was found to be reached by changing the dihedral angle of the Cα-Cβ-C3-C2 system in the W38 side chain from $-142°$ to $-93°$ in their model. The dihedral angle, $-93°$, proposed here is consistent with the fact that the tryptophan W3 band was found at 1548 cm^{-1} for *Pf*3 instead of at 1560 cm^{-1} found for *fd* above. The proposed orientation of Trp-38 was found to also allow cation-π interaction with Arg-37, which was suggested by Wen and Thomas,[17] if a proper set of changes were applied on the dihedral angles of the Arg-37 side chain from those given in the Welsh et al. model.[16] The details of this will be published shortly.

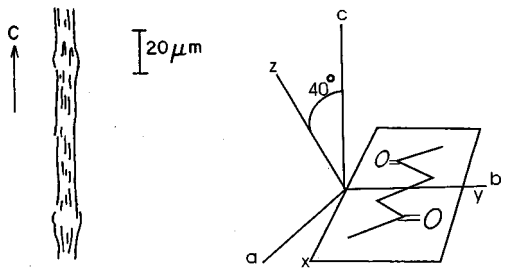

Fig. 10 (Left) Fowl feather barb. This is a reproduction of Fig. 1 in Ref. 20. (Right) Average orientation of an antiparallel chain pleated sheet in the barb (Ref. 20).

Example III. Arrangement of the Polypeptide Sheet in Fowl Feather Barb

Spectroscopic studies of feather keratin have so far been made mostly with samples prepared from the calamus or rachis section of avian feathers.[18,19] Their barbs, in which the crystallite alignment looks better under a polarizing microscope, are too thin for conventional Raman spectroscopic measurement. Due to recent developments in Raman microscopy, however, even such a thin barb (10 μm in diameter, for example) can now be subjected to vibrational spectroscopic examinations.[20]

A single barb prepared from fowl feather was found to be a long cylinder with a diameter of 10 μm and with small lumps arranged at intervals of 75 μm along its direction of elongation (Figure 10). Under a polarizing microscope it showed marked positive birefringence. The retardation looked rather homogeneous all over the cylinder. Step 1. The barb had cylindrical symmetry, and the axis was defined as the *c* axis. Step 2. Its polarized infrared spectra indicated a 1684 cm^{-1} band as well as a 1633 cm^{-1} band. Therefore, it was considered to involve an antiparallel chain pleated sheet structure.[21] Thus, determining a Raman tensor assignable to this structure was the next problem to be solved. On the basis of the Raman spectroscopic measurement on a single crystal of a dipeptide (aspartame), whose molecule involves only one peptide group, Tsuboi et al.[22] derived the shape and orientation of the amide I Raman tensor excited at 488.0 nm. By placing this tensor at every peptide group, the Raman tensor of an antiparallel chain pleated sheet was calculated. Here, the atomic coordinates given by Pauling and Corey[23] were adopted. The result of the calculation is shown in Figure 11. Step 3. The sample barb was found to be fluorescent, but irradiation with a relatively weak laser beam for 1 or 2 h rendered it less fluorescent to the extent that a Raman spectroscopic measurement became possible. Steps 3 and 4. The signal-to-noise ratio, however, did not yet become sufficiently high to observe the two components, *cc* and *ca*, separately with a polarizer. Thus, only the Raman scattering intensity, $Icc + Ica$, was obtained. Likewise, only the Raman scattering intensity $Iaa + Iac$ was examined, instead of observing *Iaa* and *Iac* separately. The results of these observations are

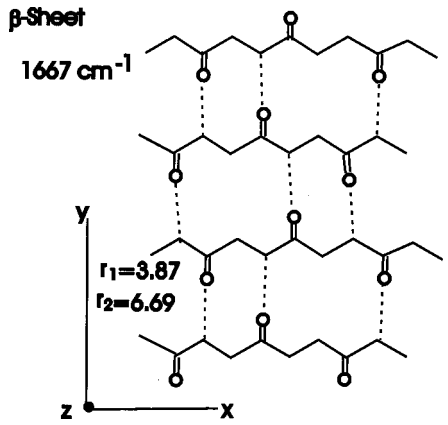

Fig. 11 Principal axes (x, y, and z) and relative magnitudes of the tensor components ($r_1=\alpha_{xx}/\alpha_{zz}$ and $r_2=\alpha_{yy}/\alpha_{zz}$) for the amide I Raman band (1667 cm^{-1}) of an antiparallel chain pleated sheet (Ref. 20).

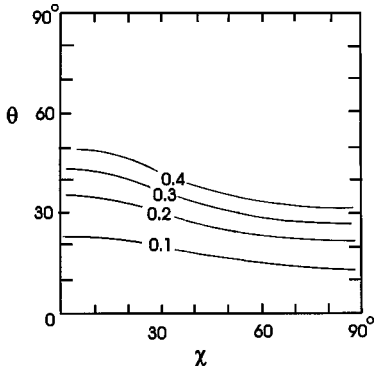

Fig. 13 Contour lines of $(Icc+Ica)/(Iaa+Iac)=0.1$, 0.2, 0.3, and 0.4 drawn in (θ, χ) space. Here $(Icc+Ica)/(Iaa+Iac)$ is the Raman scattering intensity ratio expected from the orientations (θ and χ) of the antiparallel chain pleated sheet whose principal axes are x, y, and z as shown in Fig. 11. Here, it was assumed that $r_1=\alpha_{xx}/\alpha_{zz}=3.87$ and $r_2=\alpha_{yy}/\alpha_{zz}=6.69$, as calculated by the method given in the text.

shown in Figure 12. As seen, a sharp Raman peak is found to rise at 1667 cm^{-1} in the broad background Raman scattering covering the 1690–1640 cm^{-1} range. This 1667 cm^{-1} Raman band is assigned to the amide I vibration of the antiparallel chain pleated sheet, in which all the peptide groups vibrate in phase. The broad background Raman scattering is probably caused by a disordered polypeptide portion. Step 6. As can be seen in Figure 12, the sharp 1667 cm^{-1} band is much stronger for the $Iaa+Iac$ spectrum than for the $Icc+Ica$ spectrum. This suggests that the β-sheet plane is arranged somewhat perpendicular to the barb axis (c axis). By use of Eq. (4) and a similar one for Iac/Iaa, coutour lines for several values of $(Icc+Ica)/(Iaa+Iac)$ were constructed in (θ, χ) space (Figure 13). The observed $(Icc+Ica)/(Iaa+Iac)$ value is estimated to be 2.5 ± 0.5 (Figure 12). Therefore, θ, the angle of inclination of the normal of the β-sheet plane from the c axis, must be in the range of 23°–44°. The polarized infrared spectra of seagull feather rachis observed by Fraser et al.[24] showed the transition moment of the 1634 cm^{-1} band (along the y axis in Figure 11) is nearly perpendicular to the c axis, whereas the transition moment of the 1691 cm^{-1} band (along the x axis in Figure 11) is substantially inclined away from c axis. If this is also the case for the fowl feather barb, the orientation angles are estimated as $(\theta,\chi)=(40\pm5°,0\pm10°)$. This orientation is illustrated in Figure 10. Fraser et al.[24] showed that the antiparallel chain pleated sheets must be distorted in the feather keratin, so as to conform to the ruled surface of a helix with pitch of 95 A. The average orientation derived from Raman spectroscopic work must now be accommodated to the framework of Fraser and co-workers.[24]

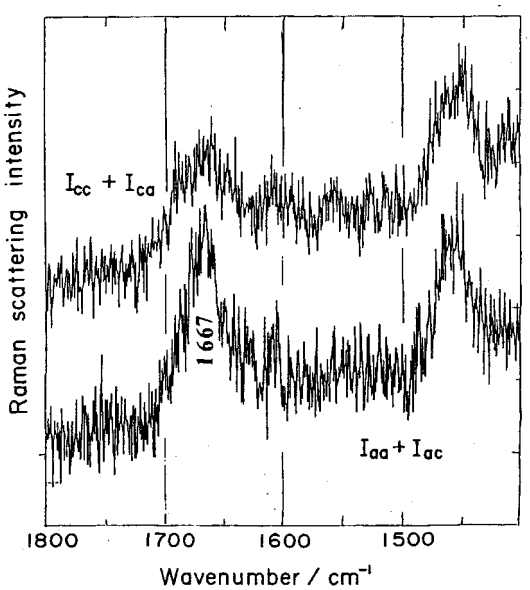

Fig. 12 Raman spectra of single barb from fowl feather (Ref. 20). (Upper spectrum) The electric vector of the exciting laser beam (488.0 nm) was placed parallel to the direction of barb elongation (c axis). The Raman scattering beam is considered to involve cc and ca components. (Lower spectrum) The exciting laser beam is polarized perpendicular to the c axis, so the Raman scattering beam consists of the aa and ac components. This is a reproduction of Fig. 3 in Ref. 20.

Concluding Remarks

In the days ahead, this method will quite often be a complementary one to the x-ray crystallographic and nuclear magnetic resonance methods used in structural biology. Some parts of the lists of atomic coordinates in the Protein Data Bank would possibly be revised through this method. In addition, this method may be useful for *in situ* examinations of biological systems that are not accessible to x-ray or nuclear magnetic resonance methods.

Acknowledgments

Much of the work reviewed here was carried out in collaboration with Professor George J. Thomas, Jr., Professor Shi-Yuan Yang, Professor Kiso Akahane, and Dr. Teruki Ikeda. The author wishes to express his sincere thanks to them.

References

1. M. Melkonian and H. Robenek, "The eyespot apparatus of flagellated green algae: A critical review," *Prog. Phycological Res.* **3**, 193–268 (1984).

2. M. Tsuboi and G. J. Thomas, Jr., ''Raman scattering tensors in biological molecules and their assemblies,'' *Appl. Spectrosc. Rev.* **32**, 263–299 (1997).
3. E. B. Wilson, Jr., J. C. Decius, and P. C. Cross, *Molecular Vibrations, The Theory of Infrared and Raman Vibrational Spectra*, p. 286, Mc Graw–Hill, New York (1955).
4. Y. Kubo, T. Ikeda, S.-Y. Yang, and M. Tsuboi, ''Orientation of carotenoid molecules in the eyespot of alga: *In situ* polarized resonance Raman spectroscopy,'' *Appl. Spectrosc.* **54**, 1114–1119 (2000).
5. S.-Y. Yang and M. Tsuboi, ''Polarizing microscopy of eyespot of *Chlamydomonas*,'' *Biospectroscopy* **3**, 93–100 (1999).
6. M. Tsuboi, T. Ueda, K. Ushizawa, Y. Ezaki, S. A. Overman, and G. J. Thomas, Jr., ''Raman tensors for the tryptophan side chain in proteins determined by polarized Raman microscopy of oriented *N*-acetyl-*L*-tryptophan crystals,'' *J. Mol. Struct.* **379**, 43–50 (1996).
7. T. Yamane, T. Andou, and T. Ashida, ''*N*-acetyl-*L*-tryptophan,'' *Acta Crystallogr., Sect. B: Struct. Crystallogr. Cryst. Chem.* **B33**, 1650–1653 (1977).
8. S. A. Overman, M. Tsuboi, and G. J. Thomas, Jr., ''Subunit orientation in filamentous virus $Ff(fd,f1,M13)$,'' *J. Mol. Biol.* **259**, 331–336 (1996).
9. M. Tsuboi, S. A. Overman, and G. Thomas, Jr., ''Orientation of tryptophan-26 in coat protein subunits of the filamentous virus *Ff* by polarized Raman microscopy,'' *Biochemistry* **35**, 10403–10410 (1996).
10. T. Miura, H. Takeuchi, and I. Harada, ''Tryptophan Raman bands sensitive to hydrogen bonding and side-chain conformation,'' *J. Raman Spectrosc.* **20**, 667–671 (1989).
11. H. Takeuchi, M. Matsuno, S. A. Overman, and G. Thomas, Jr., ''Raman linear intensity difference of flow-oriented macromolecules: Orientation of the indole ring of tryptophan-26 in filamentous virus *fd*,'' *J. Am. Chem. Soc.* **118**, 3498–3507 (1996).
12. J. W. Ponder and F. M. Richards, ''Tertiary templates for proteins: Use of packing criteria in the enumeration of allowed sequences for different structural classes,'' *J. Mol. Biol.* **193**, 775–791 (1987).
13. D. A. Marvin, R. D. Hale, C. Nave, and M. H. Citterich, ''Molecular models and structural comparisons of native and mutant class I filamentous bacteriophages $Ff(fd,f1,M13)$ $If1$ and *IKe*,'' *Mol. Biol.* **235**, 260–286 (1994).
14. M. F. Symmons, L. C. Welsh, C. Nave, D. A. Marvin, and R. N. Perham, ''Matching electrostatic charge between DNA and coat protein in filamentous bacteriophage. Fibre diffraction of charge-deletion mutants,'' *J. Mol. Biol.* **245**, 86–91 (1995).
15. M. Tsuboi, S. A. Overman, K. Nakamura, A. Rodriguez-Casasdo, and G. J. Thomas, Jr., ''Orientation of tryptophan 38 in the subunit of filamentous virus $Pf3$ determined by polarized Raman spectroscopy,'' *Biophys. J.* **78**, 395A (1999).
16. L. C. Welsh, M. F. Symmons, J. M. Sturtevant, D. A. Marvin, and R. N. Perham, ''Structure of the capsid of $Pf3$ filamentous phage determined from x-ray fibre diffraction data at 3.1 A resolution,'' *J. Mol. Biol.* **283**, 155–177 (1998).
17. Z.-Q. Wen and G. Thomas, Jr., ''Ultraviolet-resonance Raman spectroscopy of the filamentous virus $Pf3$: Interactions of Trp 38 specific to the assembled virion subunit,'' *Biochemistry* **39**, 146–152 (2000).
18. R. D. B. Fraser, T. P. MacRae, and G. E. Rogers, in *Keratins: Their Composition, Structure and Biosynthesis*, pp. 121–132, Thomas, Springfield, IL (1972).
19. S. L. Hsu, W. H. Moore, and S. Krimm, ''Vibrational spectrum of unordered polypeptide chain: A Raman study of feather keratin,'' *Biopolymers* **15**, 1513–1528 (1976).
20. M. Tsuboi, F. Kaneuchi, T. Ikeda, and K. Akahane, ''Infrared and Raman microscopy of fowl feather barb,'' *Can. J. Chem.* **69**, 1752–1757 (1991).
21. T. Miyazawa and E. R. Blout, ''The infrared spectra of polypeptides in various conformations: Amide I and II bands,'' *J. Am. Chem. Soc.* **83**, 712–719 (1961).
22. M. Tsuboi, T. Ikeda, and T. Ueda, ''Raman microscopy of a small uniaxial crystal: Tetragonal aspartame,'' *J. Raman Spectrosc.* **22**, 619–626 (1991).
23. L. Pauling and R. B. Corey, ''Two rippled-sheet configuration of polypeptide chains, and a note about the pleated sheets,'' *Proc. Natl. Acad. Sci. U.S.A.* **39**, 253–256 (1953).
24. R. D. B. Fraser, T. P. MacRae, D. A. D. Parry, and E. Suzuki, ''The structure of feather keratin,'' *Polymer* **12**, 35–52 (1971).